Journal of Ceramic Processing Research. Vol. 9, No. 3, pp. 234~239 (2008)

J O U R N A L O F
Ceramic Processing Research

Effects of the addition of minute amounts of alumina on the microstructure and sintering behavior of yttria stabilized tetragonal zirconia polycrystals ceramic via a co-precipitation process

Chih-Cheng Chen[a,b], Hsing-I Hsiang[b,*] and Chang-Min Zhou [b]

[a]*Department of Mechanical Engineering, Far East University, Tainan, Taiwan, R.O.C.*

[b]*Particulate Materials Research Center, Department of Resources Engineering, National Cheng Kung University, Tainan, Taiwan, R.O.C.*

It is feasible to add homogeneously minute amounts (0.25 wt%) of Al_2O_3 into 3 mol% yttria stabilized tetragonal zirconia polycrystals using a co-precipitation procedure to produce precursory gel nano-powders. X-ray diffraction, scanning electron microscopy, high-angle annular dark-field-field emission gun transmission electron microscopy, relative density determination, shrinkage, and resistivity measurements using impedance spectroscopy were combined to elucidate the microstructure and sintering behavior of zirconia ceramics produced using 0.25 wt% added Al_2O_3, possibly the limit of solubility of Al_2O_3 in the ZrO_2 structure. Two modes of sintering behavior may be described as: (I) The total solid solution of Al_2O_3 in the solid solution of ZrO_2 structure via a precursory co-precipitation procedure; calcining at 800 °C and sintering at 1275 °C can be shown to indicate the viable solubility of Al_2O_3 in the ZrO_2 structure, designated as stage I of the thermal treatment; and (II) At the higher sintering temperature, above 1275 °C, the segregation of Al_2O_3 at triple junction occurs. Higher bulk and grain boundary resistivity values are found for the sample sintered at 1275 °C, which probably resulted from the dissolution of Al_2O_3 in the ZrO_2 structure.

Introduction

Among the technical ceramic materials, zirconia (ZrO_2)-based and its various composite formulations have emerged to occupy the most favorable competitive position in a wide range of applications both in the engineering and electronic fields. There have been extensive studies on the subjects of processing, microstructure, properties and applications [1-3]. While the fundamental aspects have been covered; there seems to be room for some meticulous studies directed toward the fine-tuning or optimization in the preparative methodology, particularly in connection to a relatively low sintering temperature to obtain an acceptable densification in the sintered ZrO_2-based bodies. As such, we have attempted to evaluate the effect of a minute addition, namely, 0.25% Al_2O_3 on the microstructure and sintering behavior of 3 mol% yttria stabilized tetragonal zirconia polycrystals (Y-TZP) via a co-precipitation process.

It is necessary to give a brief account of the experimental design for this study. The limiting solubility of Al_2O_3 in ZrO_2 has been determined to be a minute quantity of 0.2 wt% Al_2O_3 [3, 4]. Zirconia for functional applications have been adequately presented by Guo [4] and the related defect chemistry has been evaluated by resistivity measurements for both bulk and granular boundaries. In addition to acting as a sintering aid, addition of Al_2O_3 serves a highly useful function in Y-TZP material by offering resistance to H_2O vapor degradation of ZrO_2-based bodies in the temperature range of 373-573 K [5]. A somewhat excessive addition of Al_2O_3 may give deteriorating effects on the densification [6].

The objective of this study is to obtain a particular nano-composite Y-TZP/Al_2O_3 powder formulation using a co-precipitation procedure, using a minute quantity of 0.25 wt% Al_2O_3 in the feed stock. XRD analysis of the phase evolution and shrinkage measurements using thermal treatments and the electrical resistivity were performed on the sintered bodies. Scanning electron micrographs (SEM) and high-angle annular dark-field-field emission gun transmission electron microscopy (HAADF-FETEM) images are also provided to show the microstructure of the sintered bodies. Accordingly, a discussion of the microstructure and sintering behavior of Y-TZP/Al_2O_3 (0.25 wt%) is elaborated to show the suitability of the composition and preparation procedure.

Experimentation

Sample preparation

The particular formulation of powder composition is

*Corresponding author:
Tel : 886-6-2757575 ext 62821
Fax: 886-6-2380421
E-mail: hsingi@mail.ncku.edu.tw

designated as Y-TZP-A, having a chemical composition 3 mol% yttria stabilized tetragonal zirconia polystals/ Al_2O_3 (0.25 wt%). The feed stock materials were all technical grades of $ZrOCl_2 \cdot E8H_2O$, Y_2O_3, and $Al(NO_3)_3 \cdot D9H_2O$. Homogenization was obtained by dissolution, mixing and stirring. A conventional chemical co-precipitation was completed by the addition of NH_4OH solution maintained at pH = 9.5 throughout the operation. Thorough washings of the precipitated product were performed using pure water and isopropanol. The filtered precipitated product was dried at 80 °C for 24 h in ambient atmosphere. The dried powder was finally calcined at 800 °C (heating rate of 4 K miniute^{-1}, maintained at 2 h and cooling in an oven furnace) and then compacted using a cold isostatic press at 300 MPa. The green bodies were heat treated and sintered at temperatures, of 1250 °C, 1275 °C, 1300 °C, 1325 °C, and 1350 °C, each held for 2 h.

Characterization of sintered bodies

Evolution of crystalline phases in precursor powders and sintered bodies were determined using an X-ray diffractometer (XRD) (Siemens, D5000). The crystallite sizes of each specimen were calculated using the Scherrer formula. Thermal shrinkage was measured using a dilatometer (Netzsch, DIL 420C). The densities of the sintered samples were determined using the Archimedean method. The microstructure of thermally etched cross-sections was investigated using SEM (Hitachi, S-4100). HAADF-FETEM (FEI E.O Tecnai, F20 G2 MAT S-TWIN) and energy dispersive spectroscopy (EDS) (Noran, Voyager 1000) were used to examine the microstructure and identify the phases that occurred during sintering. Electrical resistivities of the sintered bodies were measured using the impedance approach in a frequency range of 20 Hz to 1 MHz with a HP 4285 A precision LCR meter.

Results and Discussion

Crystalline phase identification

Figure 1(a) show the XRD patterns of the starting gel powder and calcined (at 800 °C) Y-TZP (without Al_2O_3) and Y-TZP-A (with 0.25 wt% Al_2O_3). Both starting gel powders, derived from co-precipitation and air-dried, are amorphous. Only the tetragonal ZrO_2 phase could be observed for both specimen types, but differing slightly in the peak heights of t-ZrO_2. The crystallite sizes measured using the Scherrer formula show that Y-TZP-A has an average size of 15.8 nm as opposed to 18.1 nm for Y-TZP (without Al_2O_3). Seemingly, the addition of even a minute amount of Al_2O_3 (0.25 wt%) has a substantial suppressive effect on the grain growth of t-ZrO_2.

Figure 1(b) shows the XRD patterns of the sintered specimen (at 1350 °C/2 h). A small amount of monoclinic ZrO_2 phase is noticeable in the Y-TZP specimen; whereas the Y-TZP-A specimen contains only pure t-ZrO_2 phase. Thus, it may be generalized that even a minute addition (0.25 wt%) of Al_2O_3 can have a significant suppressive

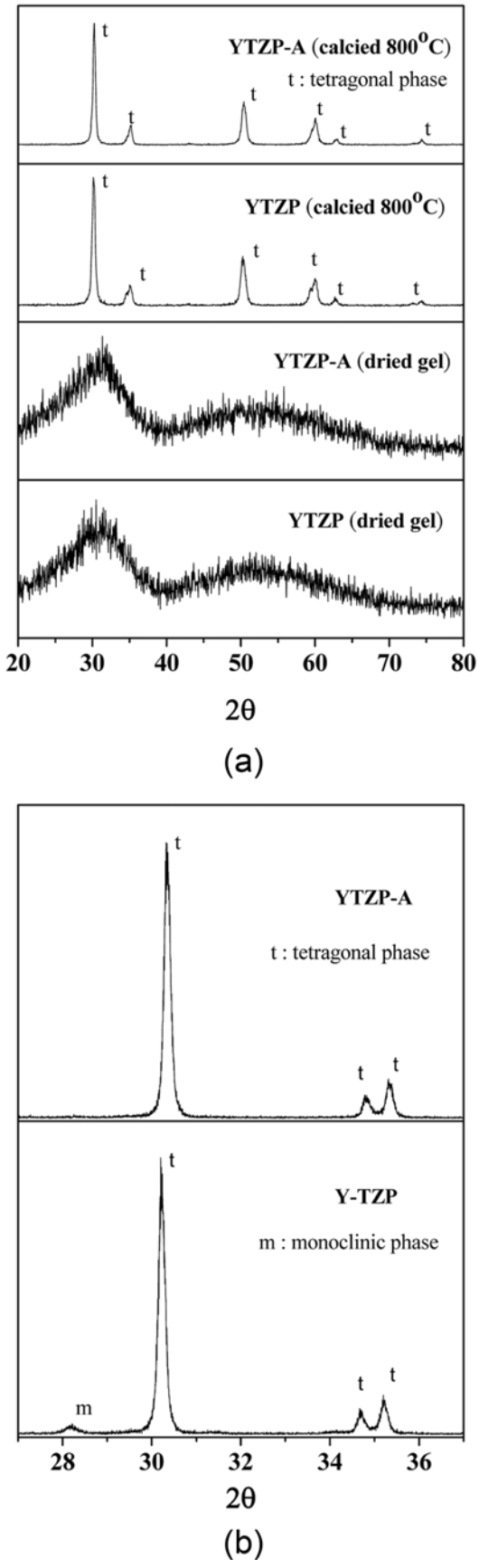

Fig. 1. (a) XRD patterns of the starting gel powder and calcined (at 800 °C) Y-TZP (without Al_2O_3) and Y-TZP-A (with 0.25 wt% Al_2O_3). (b) XRD patterns of the sintered specimen (at 1350 °C/2 h).

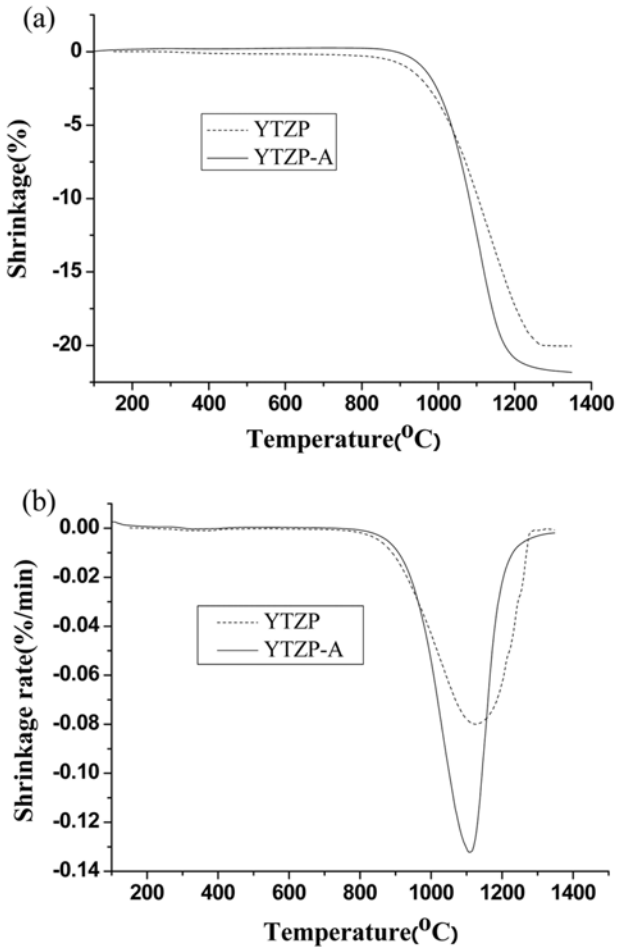

Fig. 2. (a) Shrinkage curves of the Y-TZP and Y-TZP-A samples. (b) Shrinkage rate vs. sintering temperature for the Y-TZP and Y-TZP-A samples.

effect on the phase evolution in the emergence of monoclinic ZrO_2 and on the grain growth of the tetragonal ZrO_2.

Effect of Al_2O_3 on sintering behavior

It may be noted from Fig. 2(a) that at 1300 °C the shrinkage of the sintered specimen for Y-TZP-A is slightly larger than Y-TZP by an amount of about 2.5% (linear). Figure 2(b) shows that the temperature for maximum shrinkage rate for the same occurs at a lower temperature by about 30 °C. Thus, it may be concluded that the minute addition of Al_2O_3 seems to increase the densification of the sintered bodies. Density measurement results (Table 1) also show the same trend, further proving the contention that even a minute addition of Al_2O_3 (0.25 wt%) has a beneficial effect on densification in sintering. Our results seem to more or less agree with that of Yang [3]; and that our precursory co-precipitated gel powders renders the indication that 0.25 wt% Al_2O_3 may just be within the limit of solubility of Al_2O_3 in the sintered body of Y-TZP-A.

Effect of minute Al_2O_3 addition on Y-TZP microstructure.

Figures 3(a), (b) show the HAADF-STEM images of Y-TZP-A sintered at 1275 °C and 1350 °C, respectively. In the HAADF-STEM imaging, the image intensity is approximately proportional to the square of the atomic number termed as Z-contrast imaging and atomic column occupancy, allowing heavy atoms to be visualized directly from the image contrast features. Thus, the dark regions in Fig. 3 can be attributed to Al-rich phases, as confirmed by the corresponding selective area electron diffraction pattern (SAEDP) and EDS studies and discussed later. The amount of the Al-rich phases existing in the Y-TZP-A increased as the sintering temperature was raised from 1275 °C to 1350 °C. Figure 4 shows a higher-magnification HAADF-STEM image, and SAEDP and EDS of the Y-

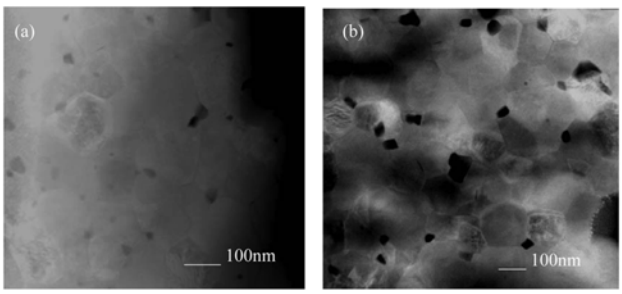

Fig. 3. HAADF images of Y-TZP-A sintered at (a) 1275 °C and (b)1350 °C.

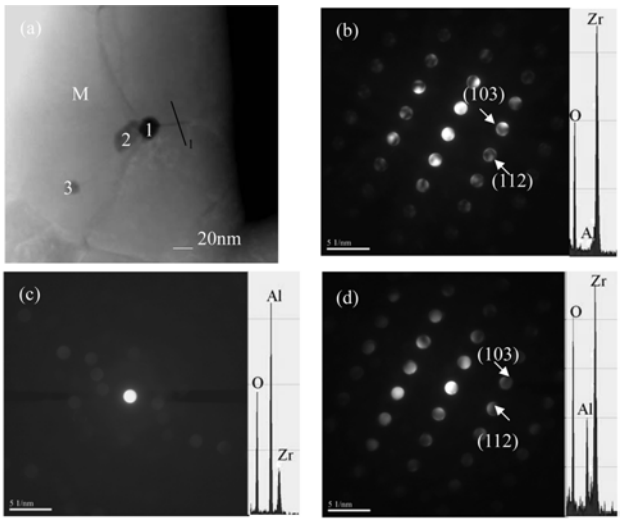

Fig. 4. (a) A higher-magnification HAADF image, and corresponding SAEDP and EDS of the Y-TZP-A sintered at 1275 °C (b) M region, (c) 1 region, (d) 2 region.

Table 1. Relative densities of Y-TZP and Y-TZP-A ceramics sintered at various temperatures

sample	Y-TZP 1275 °C	Y-TZP-A 1250 °C	Y-TZP-A 1275 °C	Y-TZP-A 1300 °C	Y-TZP-A 1325 °C	Y-TZP-A 1350 °C
Relative density	93.3%	96.8%	98.4%	97.2%	97.1%	95.7%

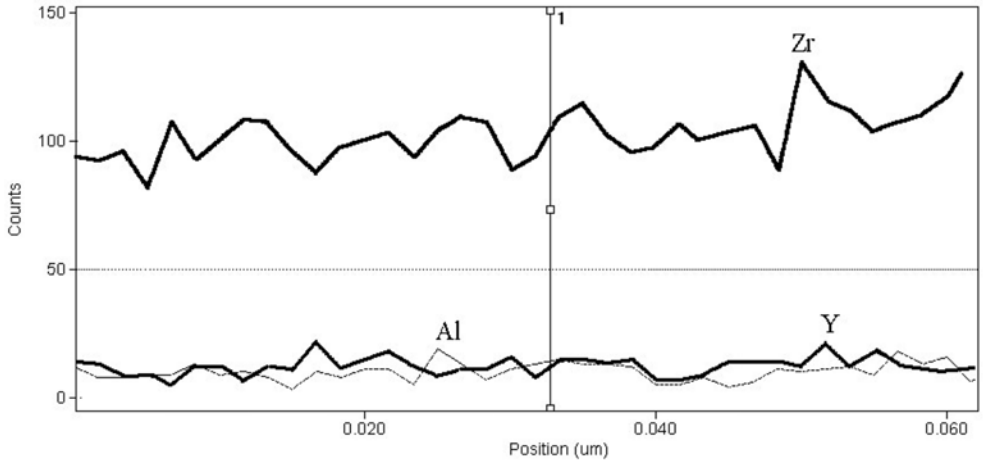

Fig. 5. Y, Al, and Zr-distribution profiles across line I in Y-TZP-A sintered at 1275 °C (Fig. 4(a)).

TZP-A sintered at 1275 °C. The microstructure is found to comprise four types of sub-regions (regions M, 1, 2, and 3). In Fig. 4(b) region M is the matrix in the Y-TZP-A sintered at 1275 °C and it is composed of t-ZrO_2, as confirmed by the SAEDP, with an overall chemical composition (atomic basis) of Zr/Al/Y = 93/1/6. Matsui [7] investigated the effect of Al_2O_3-doping on the grain boundary microstructure and phase transformation in Y-TZP and observed that no amorphous or second phase existed along grain boundary faces, but Y^{+3} and Al^{+3} ions segregated at grain boundary. Figure 5 shows Y, Al, and Zr-distribution profiles across line I in Y-TZP-A sintered at 1275 °C, and indicates no obvious Y^{+3} and Al^{+3} ions segregated at grain boundary. However, the phase (region 1 in Fig. 4(a)) at the triple junction is identified as amorphous using SAEDP. It was found to be richer in Al, with a chemical composition Zr/Al/Y = 8/92/0 (Fig. 4(c)), which is consistent with the observation reported by Vasiliev and Padture [8]. The discrepancy between our observation and that of Matsui. can be accounted for due to the different mixing homogeneity resulting from different preparation methods. Figure 4(d) shows the SAEDP, and corresponding EDS of region 2 within the matrix. The chemical composition of region 2 is found to be Zr/Al/Y = 58/35/7, and the crystal structure of the particle is identified to be t-ZrO_2, using SAEDPs and careful tilting experiments. Note that the d-spacing of (103) for t-ZrO_2 is shifted from 0.1577 nm (region M) to 0.1547 nm (region 2), indicating that Al^{+3} is in solid solution with t-ZrO_2. The chemical composition and crystal structure of region 3 are found to be Zr/Al/Y = 70/26/4, and t-ZrO_2, which are comparable to those of region 2. As the sintering temperature is raised from 1275 °C to 1350 °C, the amount of Al-rich amorphous phase at triple junctions is found to increase Fig. 3, which may result from the outward diffusion of the Al that was in solid solution with ZrO_2 [8]. The apparent density of sintered specimens seems to have slightly decreased as the temperature increases, as shown in Table 1 and the micrographs of Fig. 6. It is likely that

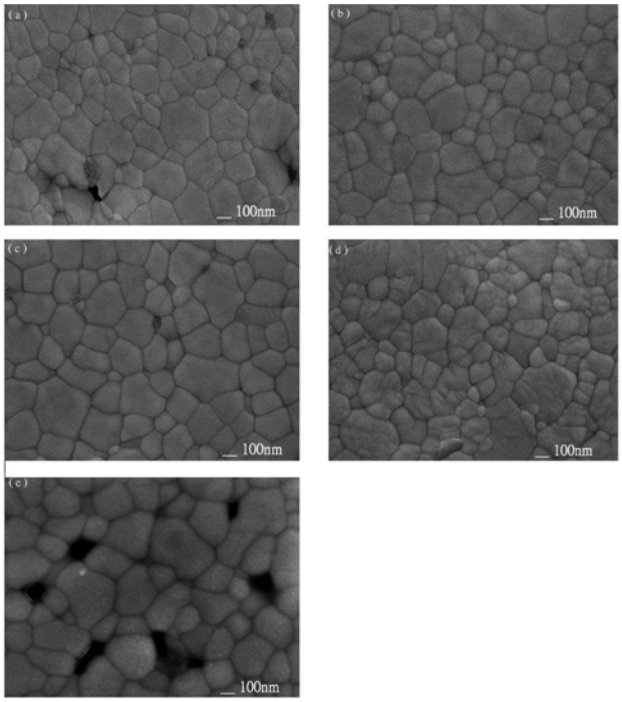

Fig. 6. SEM micrographs of the Y-TZP-A samples sintered at different temperatures: (a) 1250 °C, (b) 12750 °C, (c) 1300 °C, (d) 1325 °C, (e) 1350 °C.

the amount of the Al-rich amorphous phase which has a lower density than t-ZrO_2 increased as the sintering temperature was raised above 1275 °C leading to the lowering of the sintered density.

The Schottky-barrier model is commonly used to explain the electrical properties of zirconia ceramics, as illustrated in Fig. 7 [9, 10]. The potential of grain-boundary core of Al-doped Y-TZP is positive. The positively charger grain boundary core expels oxygen vacancies, but attracts Al^{+3} cation thereby causing the oxygen vacancy depletion in the space-charge layer [11]. Guo et al. reported that an Al_2O_3 addition within the solubility limit lightly increases the bulk resistivity, but considerably increases the grain boundary resistivity [12, 13]. Impedance spectroscopy

Table 2. Bulk and grain boundary resistivity values for Y-TZP and Y-TZP-A samples obtained by the intercept on the Z'-axis from the low-frequency impedance data at 300 °C

sample	Y-TZP (1275 °C/2 h)	Y-TZP-A (1275 °C/2 h)	Y-TZP-A (1350 °C/2 h)
Bulk resistivity (kΩ)	100	125	103
Grain boundary resistivity (kΩ)	165	520	395

has been widely applied to study grain boundary effects in the zirconia system [14]. The bulk and grain boundary resistivity values can be obtained by an impedance spectrum analysis, as shown in Fig. 8. The bulk and grain boundary resistivity values for Y-TZP and Y-TZP-A samples obtained by the intercept on the Z'-axis from the low-frequency impedance data at 300 °C are summarized in Table 2. As shown by Table 2, the sequences of the bulk and grain boundary resistivity values from high to low are as follows: Y-TZP-A sintered at 1275 °C, Y-TZP-A sintered at 1350 °C, and finally Y-TZP sintered at 1275 °C. This phenomenon can be explained by: (1) The dissolution of Al_2O_3 in the ZrO_2 structure for Y-TZP-A sintered at 1275 °C, as revealed by the TEM and EDS, increases the Schottky barrier height, thereby decreasing the oxygen vacancy concentration in the space-charge layer, which results in the higher grain boundary resistivity value. (2) For the Y-TZP-A sintered at 1350 °C, Al_2O_3 seems slowly to detach from the ZrO_2 structure and segregate at triple junctions as an amorphous phase as confirmed by TEM Fig. 3, which blocks the ionic transport by decreasing the conduction path width and constricting current lines [15], leading the grain boundary resistivity value to become higher than that of Y-TZP. (3) The formation of complex defect associates occur due to the dissolution of Al_2O_3 in the ZrO_2 structure, which binds some oxygen vacancies to immobile ions [15], thereby, increasing the bulk resistivity of the sintered Y-TZP-A specimen.

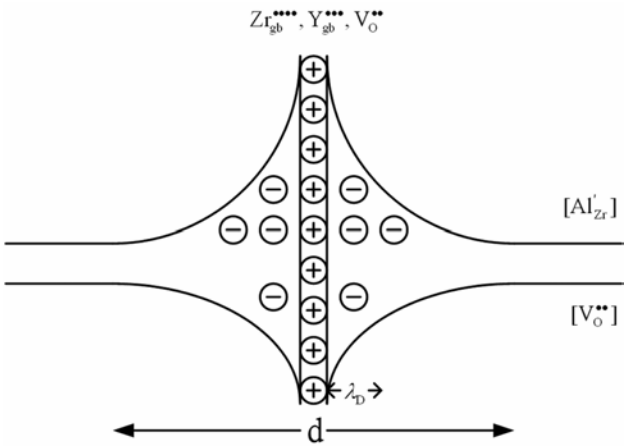

Fig. 7. Schottky-barrier model for the grain boundary of Y-TZP-A.

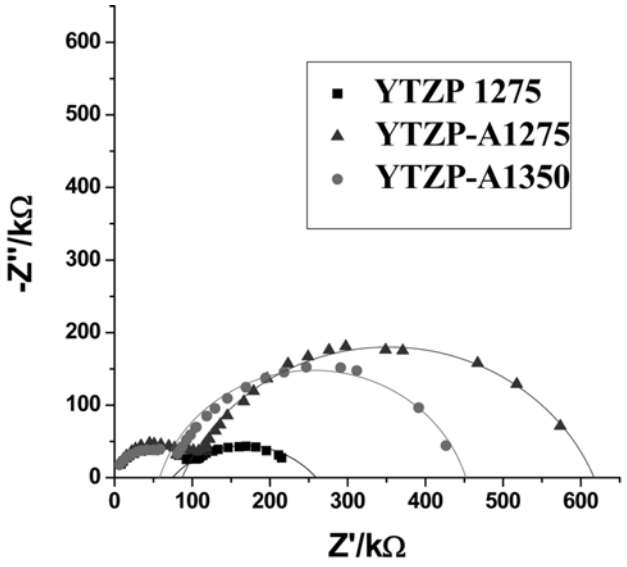

Fig. 8. Impedance spectra of the Y-TZP ceramic sintered at 1275 °C, and Y-TZP-A ceramics sintered at 1275 °C and 1350 °C.

Conclusions

Chemical co-precipitation benefits the homogeneous mixing and preparation of a minute alumina (0.25 wt%) addition to yttria stabilized tetragonal zirconia polycrystalline powder. Such a minute addition of Al_2O_3 has been shown to render two substantial effects on the yttria stabilized tetragonal zirconia polycrystalline ceramics, as (I) solid solution of Al_2O_3 in the ZrO_2 structure and (II) the segregation of Al_2O_3 as an amorphous phase at the triple junctions at a higher sintering temperature, above 1275 °C.

The dissolution of Al_2O_3 in the ZrO_2 structure for 3 mol% yttria stabilized tetragonal zirconia polystals/Al_2O_3 (0.25 wt%) sintered at 1275 °C increases the Schottky barrier height, thereby decreasing the oxygen vacancy concentration in the space-charge layer, which results in a higher grain boundary resistivity value.

As the sintering temperature of 3 mol% yttria stabilized tetragonal zirconia polystals/Al_2O_3 (0.25 wt%) is raised above 1275 °C, Al_2O_3 seems slowly to detach from the ZrO_2 structure and segregate at the triple junctions as an amorphous phase, which blocks the ionic transport by decreasing the conduction path width and constricting current lines, leading the grain boundary resistivity value to become higher than that of yttria stabilized tetragonal zirconia polystals.

Acknowledgement

This work was supported by the Ministry of Economic Affairs (92-EC-17-A-08-S1-023) through Particulate Materials Research Center of National Cheng Kung University.

References

1. J.L. Shi, J. Europ. Ceram. Soc. 15 (1995) 967-973.
2. J.K. Lee, J. Mater. Sci. Lett. 21 (2002) 259-261.
3. S.Y. Yang, Solid State Ionics. 172 (2004) 413-416.
4. X. Guo, J. Am. Ceram. Soc. 86 (2003) 1867-1873.
5. C.L. Yang, H.I Hsiang, and C.C. Chen, Ceram. Int. 31 (2005) 297-303.
6. V.V. Srdic, J. Am. Ceram. Soc. 84 (2001) 2771-2776.
7. K. Matsui, J. Mater. Res. 21 (2006) 2278-2289.
8. A.L. Vasiliev and N.P. Padture, Acta Mater. 54 (2006) 4921-4928.
9. J.S. Lee and D.Y. Kim, J. Mater. Res. 16 (2001) 2739-2751.
10. Y.M. Chiang and T. Takagi, J. Am. Ceram. Soc. 73 (1990) 3278-3285.
11. X. Guo and R. Waser, Prog. Mater. Sci. 51 (2006) 151-210.
12. X. Guo, Phys. Status Solidi A 183 (2001) 261-271.
13. X. Guo, W. Sigle, J. Fleig, and J. Maier, Solid State Ionics 154-155 (2002) 555-561.
14. J.E. Bauerle, J. Phys. Chem. Solids 30 (1969) 2657-2670.
15. X. Guo, J. Am. Ceram. Soc. 86 (2003) 1867-1873.
16. X. Guo, Solid State Ionics 80 (1995) 159-166.
17. X. Guo, J. Europ. Ceram. Soc. 15 (1995) 25-32.